Journal of Materials Chemistry

Cite this: J. Mater. Chem., 2012, 22, 14951

www.rsc.org/materials

PAPER

Fine-tuning the balance between crystallization and gelation and enhancement of CO_2 uptake on functionalized calcium based MOFs and metallogels†

Arijit Mallick,[a] Eva-Maria Schön,[b] Tamas Panda,[a] K. Sreenivas,[c] David Díaz Díaz*[bd] and Rahul Banerjee*[a]

Received 13th February 2012, Accepted 11th May 2012
DOI: 10.1039/c2jm30866e

The synthesis, structure, gas adsorption and catalytic properties of a new 3D porous, crystalline metal–organic framework (Ca-5TIA-MOF) as well as stable viscoelastic metallogels (Ca-5TIA-Gel) are reported. Remarkably, the preparation of both types of materials can be carried out starting from the same organic ligand (*i.e.* 5-(1,2,4-triazoleyl)isophthalic acid (5TIA)), divalent metal ion (*i.e.* Ca(II)) and organic solvent (*i.e.* DMF). In this particular case, the presence of water in the solvent system favors the formation of a crystalline MOF, whereas a pure organic solvent induces gelation. The characterization of the materials was carried out using a series of techniques including XRD, FT-IR, TGA, TEM, SEM, SAXS and dynamic rheology. Experimental PXRD peaks of both Ca-5TIA-xerogel and Ca-5TIA-MOF matched reasonably well with simulated PXRD, suggesting the presence of, at least, some common structural elements in the 3D networks of both xerogel and crystalline phases. Moreover, the nature of the metal counteranion was found to have a critical influence on the gelation phenomenon. To the best of our knowledge, this report describes unprecedented Ca-based LMW-metallogels, as well as the first porous Ca-based MOF, which shows adsorption capacity for CO_2 at 1 atm pressure. Interestingly, Ca-5TIA-xerogel presented 20% higher CO_2-uptake than the crystalline Ca-5TIA-MOF at 1 atm and 298 K. Both Ca-5TIA-MOF and Ca-5TIA-Gel also displayed a modest catalytic activity towards the hydrosilylation of benzaldehyde, with slightly better performance for the gel phase material.

Introduction

Metal–organic frameworks (MOFs) are porous, crystalline materials in which metal ions are linked together by multidentate, low molecular weight (LMW) organic ligands resulting in supramolecular coordination polymers of different topologies.[1] Over the past few years, research on MOFs has rapidly drawn considerable attention due to their promising applications in gas storage,[1a,2] separations,[2o,3] heterogeneous catalysis,[4] drug delivery[5] and sensors.[6] The practical attractiveness of MOFs mainly relies on their uniform channels, high porosities, excellent thermal stability and chemical tailorability.[7] However, the brittle nature of these crystalline materials can pose a challenge to their industrial processing and combination with other functional materials without pore blocking and/or decrease of the inner surface area.[8] In this sense, it has been suggested that viscoelastic metallogels[9] could overcome, at least partially, this limitation[10] for high-tech applications in a number of fields such as catalysis,[4g,11] photophysics,[12] sensing,[13] magnetic materials,[14] redox responsiveness,[15] and electron emission.[16] In particular, the catalytic potential of wide-ranging metallogel-based materials[9k,17] relies on two major aspects: (1) their two-phase nature, which may facilitate recovering and recycling and (2) a much higher accessibility of small reagents to the highly solvated 3D porous network in comparison to several standard heterogeneous catalysts.

Despite a substantial volume of literature on MOFs and catalytic metallogels, reports on calcium-based porous 3D MOFs are rather limited when we critically compare them with other metals.[18] Among the most recent examples, catalytically active Ca-based MOFs have been prepared using 4,4′-(hexafluoroisopropylidene) bis(benzoic acid)[18l] or anthraquinone-2,6-disulfonate[18k] as ligands. Lin and co-workers[18l] have also reported a series of new 3D MOFs made from aromatic carboxylic acids and Ca(II) ions under different conditions, which undergo remarkable destruction/construction structural transformations involving a break and reformation of the Ca–O bond. From the sustainability point of view, calcium is non-toxic and highly abundant in nature (3.4% of Earth's crust), which makes it one of the cheapest commercially

[a]*Physical/Materials Chemistry Division, CSIR-National Chemical Laboratory, Dr. Homi Bhabha Road, Pune-411008, India. E-mail: r.banerjee@ncl.res.in; Fax: +91-20-25902636; Tel: +91-20-25902535*
[b]*Institut für Organische Chemie, Universität Regensburg, Universitätsstr. 31, 93040 Regensburg, Germany. E-mail: David.Diaz@chemie.uni-regensburg.de; Fax: +49-941-9434121; Tel: +49-941-9434373*
[c]*Complex Fluids and Polymer Engineering, Polymer Science & Engineering Division, CSIR-National Chemical Laboratory, Dr. Homi Bhabha Road, Pune-411008, India*
[d]*ISQCH, Universidad de Zaragoza-CSIC, 50009 Zaragoza, Spain*
† Electronic supplementary information (ESI) available. CCDC 846548. For ESI and crystallographic data in CIF or other electronic format see DOI: 10.1039/c2jm30866e

available metals without associated environmental hazards.[19] Here we report the synthesis, characterization, gas uptake and catalytic properties of a new self-assembled porous Ca-based 3D MOF (Ca-5TIA-MOF) as well as stable Ca-based metallogels (Ca-5TIA-Gel), both synthesized from 5-(1,2,4-triazoleyl) isophthalic acid (5TIA) as the LMW organic ligand and Ca(II) as the metal ion.

Experimental section

General remarks

All reagents and solvents (p.a.) for synthesis and analyses were commercially available and used as received without further purification. Fourier transform infrared (FT-IR) spectra were taken on a Bruker Optics ALPHA-E spectrometer with a universal Zn–Se ATR (attenuated total reflection) accessory in the 600–4000 cm^{-1} region or using a Diamond ATR (Golden Gate). Thermo-gravimetric analyses (TGA) were carried out on a TG50 analyzer (Mettler-Toledo) or a SDT Q600 TG-DTA analyzer under a N_2 atmosphere at a heating rate of 10 °C min^{-1} within a temperature range of 20–800 °C. Low-pressure gas adsorption experiments (up to 1 bar) were performed on a Quantachrome Quadrasorb automatic volumetric instrument. 5-(4*H*-1,2,4-Triazol-4-yl) isophthalic acid (5TIA) was synthesized and purified following the previously reported procedure.[21] UV-Vis spectra were recorded using a PerkinElmer Lambda-35 UV-Vis spectrometer. Steady state fluorescence emission was performed using a Fluorolog HORIBA JOBIN VY fluorescence spectrophotometer. For 5TIA, a 0.01 M solution in DMF was used for UV measurements. For Ca-5TIA-Gel, either coating the material on a quartz plate or dispersing it in DMF provided the same results. For the dispersion, 12 mg of Ca-5TIA-Gel were placed into 5 mL of DMF and the mixture diluted twice. Some gel preparations were carried out using a VWR™ ultrasonic cleaner (USC200TH). Whatman® glass microfiber filters (GF/A) were used for recovering the catalyst. Analyses of the reactions were carried out by gas chromatography (GC) using a HP 5790-A GC equipped with a FID detector and a capillary column OV-1 (oven temperature: 250 °C, carrier gas: helium, internal standard: *n*-dodecane). TLC was facilitated by the use of phosphomolybdic acid stain solution in addition to UV light (254 nm) with fluorescent-indicating plates (aluminium sheets precoated with silica gel 60 F_{254}, Merck). SEM images were obtained with a Zeiss DSM 950 scanning electron microscope and FEI, QUANTA 200 3D Scanning Electron Microscope with tungsten filament as the electron source operated at 10 kV. The samples were sputtered with Au (nano-sized film) prior to imaging by a SCD 040 Balzers Union as well as by sprinkling the xerogel powder on carbon tape. TEM images were recorded using a FEI Tecnai G2 F20 X-TWIN TEM at an accelerating voltage of 200 kV. The TEM samples were prepared by dropcasting the sample of 10^{-3} M concentration from isopropanol on a copper grid TEM Window (TED PELLA, INC. 200 mesh).

Synthesis

Ca-5TIA-MOF

5TIA (44.6 mg, 0.2 mmol) and $Ca(OAc)_2$ (31.6 mg, 0.2 mmol) were mixed in a 5 mL glass vial containing 3 mL of DMF : H_2O (v/v, 1 : 1). The vial was capped and the mixture sonicated for 30 minutes at RT. This vial was kept in an oven at 85 °C for 48 h. After this time, colourless plate-like crystals were obtained, which were filtered off using Whatman filter paper and washed thoroughly with 99.9% as received EtOH. The so-obtained MOF $[Ca_2(5TIA)_2(H_2O)_2 \cdot DMF]$ (22.7 mg, 72% yield) was dried at RT under an air atmosphere (60 min): FT-IR (KBr, thin film) $\nu_{max}(cm^{-1})$: 3216 (m, br), 1670 (m), 1616 (m), 1550 (s), 1450 (m), 1381 (s), 1297 (w), 1244 (m), 1170 (w), 1085 (m), 1043 (w), 900 (w), 773 (m), 740 (m), 683 (m); elemental analysis calcd (%) for activated sample ($C_{10}H_4N_3O_5Ca$): C, 40.24; H, 1.96; N, 21.82; found: C, 39.20; H, 1.99; N, 22.24.

Ca-5TIA-Gel

$Ca(OAc)_2$ (31.6 mg, 0.2 mmol) and 5TIA (0.2 mmol, 44.6 mg) were placed into a 5 mL glass vial. Then, 2 mL of as received DMF was added and the mixture sonicated for *ca.* 15 min until it turned into homogeneous white colored solution. Finally, the solution was kept at different temperatures (*i.e.* 30 °C, 60 °C, 90 °C and 120 °C) for 2 days. In each case, white colour gels were obtained after this time. These materials should be stored in the dark: FT-IR (KBr, thin film) ν_{max} (cm^{-1}): 3349 (m, br), 1617 (m), 1550 (s), 1436 (m), 1386 (s), 1297 (w), 1248 (m), 1168 (w), 1096 (m), 1051 (w), 900 (w), 773 (m), 731 (m) and 669 (m) cm^{-1}.

UV-Vis studies

For 5TIA, a 0.01 M solution in DMF was used for the measurements. For Ca-5TIA-Gel, either coating the material on a quartz plate or dispersing it in DMF provided the same results. For the dispersion, 12 mg of Ca-5TIA-Gel were placed into 5 mL of DMF and the mixture diluted twice. Time dependent UV measurements were done by coating the gel on a quartz plate.

Single crystal X-ray diffraction

Single crystal data were collected on a Bruker *SMART APEX* three circle diffractometer equipped with a *CCD* area detector (Bruker Systems Inc., 1999a)[20] and operated at 1500 W power (50 kV, 30 mA) to generate Mo K_α radiation ($\lambda = 0.71073$ Å). The incident X-ray beam was focused and monochromated using Bruker Excalibur Gobel mirror optics. A single crystal of the MOF was mounted on a nylon CryoLoop (Hampton Research) with Paratone-N (Hampton Research). Data were integrated using Bruker *SAINT* software[21] and subsequently corrected for absorption using the program *SADABS*.[22] Space group determinations and tests for merohedral twinning were carried out using *XPREP*.[23] In this case, the highest possible space group was chosen. The structure was solved by direct methods and refined using the *SHELXTL 97* software suite.[24] Atoms were located from iterative examination of difference F-maps following least squares refinements of the earlier models. Hydrogen atoms were placed in calculated positions and included as riding atoms with isotropic displacement parameters 1.2–1.5 times $U_{eq.}$ of the attached C atoms. Data were collected at 298(2) K. The structure was examined using the *ADDSYM* subroutine of *PLATON*[25] to assure that no additional symmetry could be applied to the models. Unless noted otherwise, all

ellipsoids in *ORTEP* diagrams are displayed at the 50% probability level (see ESI†). CCDC 846548.

Powder X-ray diffraction (PXRD)

Powder X-ray diffraction (PXRD) patterns were recorded on a Phillips PANalytical diffractometer for Cu K_α radiation (λ = 1.5406 Å), with a scan speed of 2° min^{-1} and a step size of 0.02° in 2θ at RT.

Gas adsorption measurements

Low-pressure volumetric gas adsorption measurements were performed at 77 K for N_2, maintained by a liquid nitrogen bath, with pressures ranging from 0 to 760 Torr on a Quantachrome Quadrasorb automatic volumetric instrument. CO_2 adsorption measurements were carried out at 298 K within the same pressure range. Ultra high-purity H_2 was obtained by using calcium aluminosilicate adsorbents to remove trace amounts of water and other impurities before introduction into the volumetric system. The colourless microcrystals of the MOF were soaked in a dried CH_2Cl_2 : MeOH (v/v, 1 : 1) mixture for 12 h. Freshly dried CH_2Cl_2 : MeOH (v/v, 1 : 1) mixture was subsequently added and the crystals were kept for an additional 48 h to remove free solvates present in the framework. The so-obtained material was dried under vacuum (<10^{-3} Torr) at RT overnight. The samples were heated under dynamic vacuum at 60 °C (12 h) to remove the solvent present on the surface and then further heated to 100 °C (12 h) to remove the coordinated solvent molecule (water). Upon heating, Ca-5TIA-Gel retains its framework.

Rheology

Rheology was performed using a TA-ARES rheometer equipped with a force rebalance transducer. All measurements were repeated to confirm their reproducibility. A Couette geometry was used for the measurement with cup and bob diameters of 27 and 25 mm and a height of 30 mm, respectively. Strain sweep measurements were initially performed to estimate the smallest strains at which reasonable torque values, about ten times the resolution limit of the transducer, could be obtained. Subsequently, frequency sweep measurements were performed in dynamic mode, on the gel, as a function of ageing time (frequency range = 10^{-2} to 10^2 rad s^{-1}; strain = 1%). The gel was prepared in a vial and then transferred to the cup of the rheometer geometry. To prevent solvent evaporation over the period of the experiment, we added a small quantity of low viscosity fluorinated oil on the top of the sample, to act as an evaporation barrier. We confirmed that this oil is effective in preventing solvent evaporation during the experiment. To obtain a well-defined initial state for the gel, we pre-shear the gel (10 rad s^{-1} for 62.8 s) to break up the structure. We define the time at the end of the pre-shear as zero time and examine the effect of ageing from that time onwards.

SAXS

SAXS was performed using a Bruker Nanostar system, equipped with a rotating anode copper source (Cu K_α radiation), three pinhole collimation and a HiStar® multiwire detector. The X-ray path from the source to the sample chamber and from the sample chamber to the detector was evacuated. The detector q-range was calibrated using silver behenate standards. The 2D data were observed to be isotropic and were converted into an azimuthally averaged 1D data (I *vs.* q) using the Bruker software. Scattering from an empty capillary was subtracted from the data before presentation. The sample was loaded into 2 mm X-ray capillaries, and the time dependent data were collected every hour at 30 °C.

Catalytic activity

The catalytic ability of the materials was tested using the Lewis-acid catalyzed hydrosilylation of benzaldehyde with diphenylsilane as a model reaction. In a typical experiment, a solution of benzaldehyde (10.6 mg, 0.1 mmol) and diphenylsilane (36.9 mg, 0.2 mmol) in dried and degassed DMSO (1.0 mL) was gently stirred in the presence of the MOF-based catalyst (10 mol% with respect to benzaldehyde) at 65 ± 5 °C under an argon atmosphere. The reaction mixture was monitored over time by TLC and GC analysis (10 μL aliquots were transferred into an Eppendorf tube, quenched with water and extracted with Et_2O prior to injection into the GC). For recovery and recycling studies, a metallogel-based catalyst (bulk gel or xerogel) was packed in a borosilicate glass fiber filter paper and stapled to provide padlocking. After each cycle, the catalyst was washed with fresh DMSO, centrifuged and dried under high vacuum at 50 °C. $TOF_{1/2}$ (h^{-1}) is the average turn-over frequency calculated from the reaction time corresponding to 50% conversion. TOF is defined here as the molar ratio of converted substrate to catalyst per hour.

Results and discussion

In general, the synthesis of MOFs involves the combination of metal ions (connectors) and organic polyanions (linkers) with strong coordination ability toward metals (*e.g.* carboxylates, phosphonates, sulfonates). Among these linkers, aromatic carboxylates constitute useful building blocks for the synthesis of stable MOFs due to the considerable rigidity imparted by the organic ligand. On the other hand, it has been established that cooperative stabilization provided by a combination of hydrogen bonding, π–π and metal–ligand interactions is a powerful approach for the synthesis of gel-phase materials.[26] In this sense, we recently focused our attention on a 1,2,4-triazole-containing ligand (5TIA)[27a] for the construction of new Mn-MOFs showing template-based structural conversions.[27b] The versatile coordination modes of this *N*-heterocyclic carboxylic acid ligand are given by the presence of both nitrogen and oxygen donor atoms in the structure, which favour the coordination with soft- and hard-metals respectively[28] allowing the preparation of a number of functional heterometallic coordination polymers.[29] We have now found that the use of soft metals like calcium in combination with 5TIA allows the formation of either MOF (Ca-5TIA-MOF) or metallogels (Ca-5TIA-Gel), where the solvent composition plays a key role.

Synthesis of Ca-5TIA-MOF and Ca-5TIA-Gel

The synthesis of plate-like colourless crystals of Ca-5TIA-MOF was carried out using $Ca(OAc)_2$ and 5TIA as the ligand in

a mixture of DMF : H_2O (v/v, 1 : 1) at 90 °C. In contrast, when pure DMF was used as the liquid phase a fast and complete gelation was observed (Fig. 1). The gelation time upon sonication at RT was established to be 30 ± 5 min for a gelator system concentration of 0.2 M. The material was stable (*viz.* did not flow) by the "test-tube inversion" method[30] and the gel nature was further confirmed by dynamic rheological measurements (*vide infra*). It is widely accepted that the solvent molecules in gel materials are immobilized by capillaries and other related forces in the 3D network structures.[9] As 5TIA alone is unable to gel DMF, its rapid coordination with Ca(II) plays a key role in the gelation phenomenon, leading to the growth of coordination polymeric species, which undergo further entanglement in order to develop the 3D gel network. The MOF was characterized by single crystal X-ray diffraction. The experimental PXRD peaks of both Ca-5TIA-xerogel and Ca-5TIA-MOF matched well with simulated PXRD. This suggests the presence of, at least, some common structural elements in the 3D networks of both xerogel and crystalline Ca-5TIA-MOF phases (*vide infra*).

Stable non-thermoreversible Ca-5TIA-Gel could also be obtained at different temperatures ranging from room temperature (RT) to 150 °C (Fig. 2). A pH range between 6 and 8 was also found to be optimum for the gel formation. Interestingly, both optical and microstructures of the materials were found to be influenced by the processing temperature. For instance, bright pinkish gels were usually obtained at RT (Fig. 2b), whereas yellowish materials were obtained at 120 °C (Fig. 2e). Regardless of the processing temperature, ultrasonic pre-treatment of the mixture [$Ca(OAc)_2$ + 5TIA] in the appropriate solvent usually provided more homogeneous gel samples. The minimum gelation concentration (MGC) for the equimolar mixture [$Ca(OAc)_2$ + 5TIA] in DMF was established as 0.1 M. This result indicates that up to *ca.* 258 molecules of solvent are immobilized per molecule of ligand. To check the effect of water in gel formation, we varied the volume of water from 0.1 mL to 2.0 mL. A ratio H_2O : DMF of 1 : 20 (v/v) was established as the limit, above which no gelation but crystallization takes place (Section S2, Table S1 in the ESI†). This result also confirms the so-called "delicate balance" existing between these two phenomena.[31]

Solubility and gelation properties

The gelation ability of the gelator system [$Ca(OAc)_2$ + 5TIA] was evaluated for various solvents upon sonication at RT for 15 min at concentrations of the gelator system ranging between 0.1 and 0.5 M. We found that stable gels could be prepared in at least five solvents: DMF, DMSO, DMA, Quinoline and DEF (entries 2–5, 10) (Fig. 2g). Water (entry 1) afforded a clear solution of both the ligand and the metal salt, whereas the gelator system was found to be insoluble in the rest of the tested solvents. It has been established that Kamlet–Taft parameters[32] account for specific interactions between solvent and gelator molecules.[33] The α parameter defines the hydrogen bond donor ability of the solvent, which is of special importance in 3D networks built by hydrogen bonding. The β parameter represents the hydrogen bond acceptor ability and can be associated with the thermal stability of the gel, whereas the π^* parameter accounts for the polarisability and plays a key role in solvation processes during the gelation phenomenon. In our particular case, and from the results of Table 1, it is obvious that those solvents with very low α values and high β and π^* values simultaneously provided an optimal environment for the gelation process leading to highly thermally stable gels. Thus, solvents that cannot (or have a very low tendency) donate hydrogen bonds to the gelator and have low or moderate hydrogen bond acceptor ability and/or polarisability (entries 11–22) resulted in incompatible phases. On the other hand, solvents with high α values dissolve the gelator system (entry 1) or have a considerable tendency to dissolve it (entries 7–9) regardless of the β and π^* parameters. An exception to the rule was found with an ionic liquid (entry 6), which afforded partial gelation in spite of its moderate α value and low β value.

Ca-5TIA-Gel was found to be stable on standing at RT under dark conditions at least for 1.5 months. With the idea in mind of further testing the potential catalytic activity of Ca-5TIA-Gel, its stability over time (up to 5 days) in the presence of other solvents was qualitatively evaluated for the gel prepared in DMF at RT upon sonication. Small pieces of the gel were placed in glass vials and covered with different solvents. In general, the gel suffered

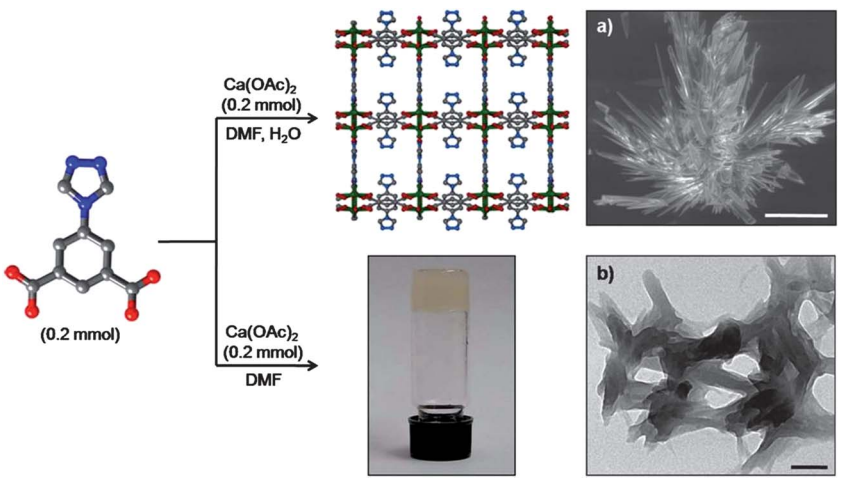

Fig. 1 Schematic diagram showing the synthesis of Ca-5TIA-MOF (*top*) and Ca-5TIA-Gel (*bottom*) under different conditions. (a) SEM image of Ca-5TIA-MOF (scale bar = 100 μm). (b) TEM image of Ca-5TIA-Gel (scale bar = 100 nm).

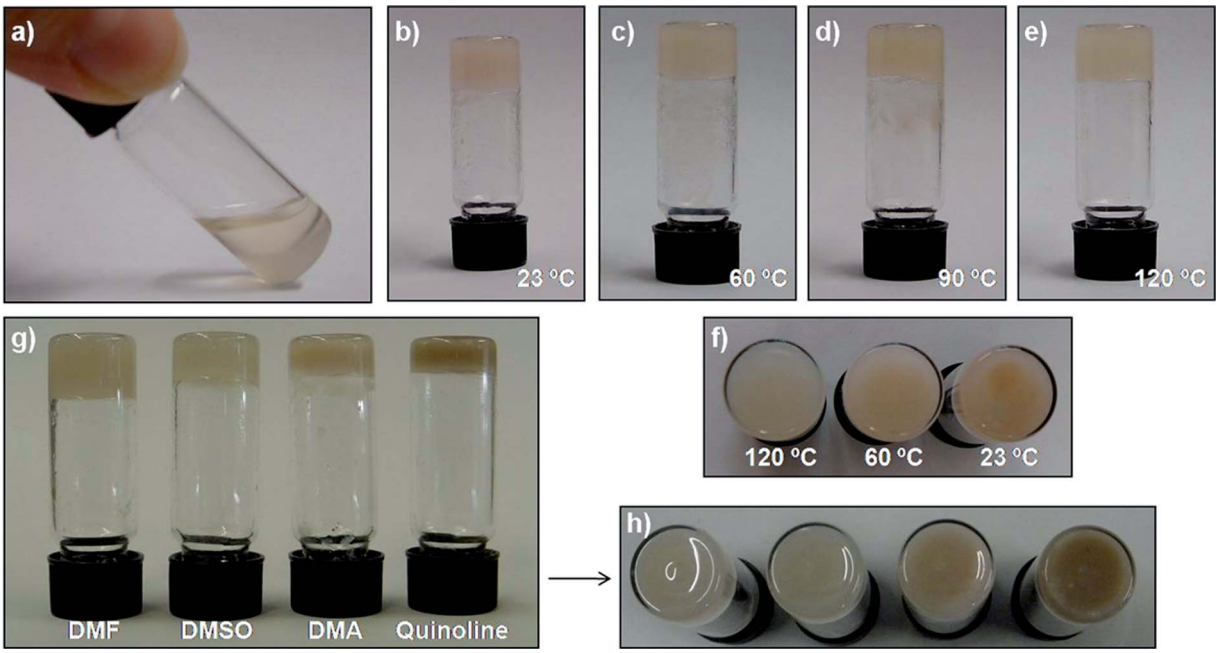

Fig. 2 (a) Digital photograph of the milky solution obtained by mixing 0.1 mmol $Ca(OAc)_2$ and 0.1 mmol 5TIA in 1 mL DMF upon sonication at RT for 15 min. Gel formation after (b) standing at RT or heating at (c) 60 °C, (d) 90 °C, (e) 120 °C in an oil bath for 2 h. (f) Top-view of upside-down vials containing the gels prepared at 23 °C, 60 °C and 120 °C. (g) Gels prepared in DMF, DMSO, DMA and Quinoline at 0.5 M concentration in the gelator system. (h) Top-view of samples.

fragmentation if shaken vigorously in the presence of other solvents, suggesting a rigid rather than a flexible supramolecular network. The results indicate that only external water can dissolve the gel, whereas strong acidic (1.0 M HCl) or basic (1.0 M NaOH) aqueous solutions caused precipitation after 24 hours. Partial fragmentation of the gel body into smaller pieces

Table 1 Gelation ability in various solvents for the system [$Ca(OAc)_2$ (0.1 mmol) + 5TIA (0.1 mmol)][a]

						Kamlet–Taft parameters		
Entry	Solvent	Result[b]	Conc.[c]	Time[d]	Gel-phase colour	α	β	π^*
1	H_2O	S	0.2–0.5	—	—	1.17	0.47	1.09
2	DMF	G	0.2	30 ± 5 min	Light pinkish	0.00	0.69	0.88
3	DMSO	G	0.4	10 ± 5[e] min	Light brownish	0.00	0.76	1.00
4	DMA	G	0.67	24–48[f] h	Light pinkish	0.00	0.76	0.88
5	Quinoline	G	0.5	10 ± 5[e] min	Brownish	0.00	0.64	0.92
6	[BMIM] $[PF_6]$	G + P	0.2–0.5	—	White	0.63	0.21	1.03
7	MeOH	I[g]	0.2–0.5	—	—	0.98	0.66	0.60
8	EtOH	I[g]	0.2–0.5	—	—	0.86	0.75	0.54
9	i-PrOH	I[g]	0.2–0.5	—	—	0.76	0.84	0.48
10	DEF	G	0.5	90 ± 5 min	—	—[h]	—[h]	—[h]
11	Acetone	I	0.2–0.5	—	—	0.08	0.43	0.71
12	THF	I	0.2–0.5	—	—	0.00	0.55	0.58
13	*n*-Hexane	I	0.2–0.5	—	—	0.00	0.00	−0.04
14	Et_2O	I	0.2–0.5	—	—	0.00	0.47	0.27
15	1,4-Dioxane	I	0.2–0.5	—	—	0.00	0.37	0.55
16	Cyclohexane	I	0.2–0.5	—	—	0.00	0.00	0.00
17	EtOAc	I	0.2–0.5	—	—	0.00	0.45	0.55
18	CH_2Cl_2	I	0.2–0.5	—	—	0.13	0.10	0.82
19	$CHCl_3$	I	0.2–0.5	—	—	0.20	0.10	0.58
20	Benzene	I	0.2–0.5	—	—	0.00	0.10	0.59
21	Toluene	I	0.2–0.5	—	—	0.00	0.11	0.54
22	CH_3CN	I	0.2–0.5	—	—	0.19	0.40	0.75

[a] Upon sonication at RT for 15 min. After this time, the temperature of the bath was 27 ± 1 °C. Additional heating with a "heat gun" was necessary only to prepare the isotropic solution of the IL. [b] Abbreviations: S = solution; G = gel; I = insoluble (upon sonication with or without further heating with a "heat gun"); P = precipitate. [c] Molar concentration (or range of concentrations in the cases where no stable gels were obtained) of the mixture [5TIA + $Ca(OAc)_2$] employed for the gelation tests (unit mol L^{-1}). [d] Time required for complete gelation at the given concentration. [e] Gelation occurred during sonication. [f] Sonication was applied for 30 min at 50 °C. [g] A white viscous blend was obtained. [h] Unknown value.

was observed on standing in most of the organic solvents after 1 h in the following order: MeOH ~ THF ~ CH_2Cl_2 ~ toluene ~ acetone > 1,4-dioxane ~ CH_3CN ~ EtOAC ~ DMF ~ Et_3N. In $CHCl_3$, the gel was stable up to 3 h. In contrast, the bulk gel was found to be fairly stable at least up to 5 days in the presence of DMSO, toluene, cyclohexane, *n*-hexane and Et_2O, which points out that some of these solvents could be a good choice for catalytic experiments (*vide infra*). Among these solvents, the gel embedded in DMSO clearly exhibited the highest resistance to mechanical stirring. Moreover, an evident change in the refraction index of the material occurs in the presence of Et_2O (the gel body becomes more white-opaque), which is not observed with the other solvents.

The light pinkish opaque Ca-5TIA-Gels remained stable to the "test-tube inversion" method but experienced a clear colour intensification over time when exposed to visible light (Fig. 3d). We found that this change in the optical properties can be inhibited under dark conditions, which may suggest intra-ligand or ligand–metal charge transfer episodes during light exposure. To gain additional insight into this process, we measured UV-Vis and fluorescence spectra of Ca-5TIA-Gel at RT and different ageing times. The UV-Vis spectrum of the ligand in DMF displayed only a broad absorption at 346 nm, which may be assigned to an intraligand orbital transition from *n* to π* and π to π* (Fig. 3a). In contrast, Ca-5TIA-Gel showed the major phenyl ring absorption peak at 290 nm and a minor hump at 346 nm probably due to unreacted ligands (Fig. 3c). A remarkable decrease in intensity of the peak at 290 nm with increasing exposure time to light points out the blockade of π to π* or *n* to π* transitions between the conjugated aromatic moiety and the lone-pair electrons of the triazole unit or the unsaturated bonds of the carbonyl groups (–COOH). On the other hand, the intense fluorescence emission concentrated at 356 nm is most likely a product of intraligand fluorescent emission as is also observed for the free ligand (Fig. 3c). The signal intensity pattern points out that the fluorescence emission of the system is quenched due to metal coordination.

Moreover, a series of studies were carried out to determine the influence of the metal counteranion on the gelation phenomenon. Interestingly, we found that the acetate anions could be efficiently exchanged by hydroxides and oxides (*i.e.* using $Ca(OH)_2$ and CaO instead of $Ca(OAc)_2$) in the gel formulation). In contrast, the use of other hard anions like chloride, carbonate, sulfate or nitrate led to the formation of either clear solutions or amorphous precipitates upon sonication at room temperature.[34] These results indicate that the counteranion plays an important role in the supramolecular assembly of the Ca–5TIA complex in solution as has been observed for other metallogels.[29a,35] We observed that experimental PXRD peaks of both Ca-5TIA-xerogel and Ca-5TIA-MOF matched reasonably well with simulated PXRD of Ca-5TIA-MOF, suggesting the presence of, at least, some common structural elements in the 3D networks of both xerogel and crystalline phases. However, the PXRD peaks of the xerogels obtained from $Ca(OH)_2$ and CaO do not match with the simulated PXRD patterns of Ca-5TIA-MOF; albeit it is noteworthy that the PXRD patterns of the $Ca(OH)_2$– and CaO-based xerogels match well with each other, which indicates some structural similarities of these two gel materials (see Section S15 in the ESI†).

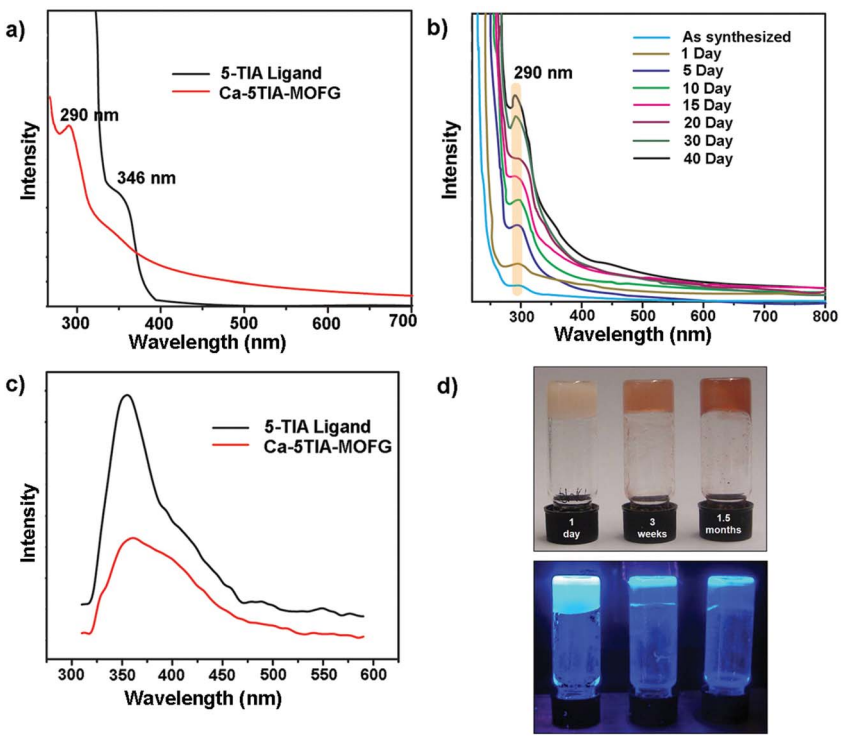

Fig. 3 (a) UV-Vis spectra for 5TIA ligand (black) and Ca-5TIA-Gel (red). (b) Time dependent UV-Vis spectra for Ca-5TIA-Gel. (c) Fluorescence emission spectra for 5TIA ligand (black) and Ca-5TIA-Gel (red). (d) (Top) Digital photograph of the Ca-5TIA-Gel made in DMF after 1 day, 3 weeks and 1.5 months; (bottom) digital photograph of the same gels under UV irradiation.

Structural analysis

The Ca-5TIA-MOF crystallizes in space group *Cmca* and structural determination by X-ray single crystal diffraction reveals a well-defined 3D network of Ca(II) linked by 5TIA ligands. The asymmetric unit of Ca-5TIA-MOF consists of only one crystallographically independent Ca(II) ion having eight coordination sites. Within the framework, each Ca(II) is surrounded by one nitrogen atom (from the triazole-*N* functionality) and six oxygen atoms (O1, O2, O3, O4, O1A and O4A) from four carboxylate groups of 5TIA ligands and one coordinated water molecule. 5TIA ligand adopts two types of binding modes in Ca-5TIA-MOF. In the first case, 5TIA is hexadented and all its carboxylate and triazole functionalities are coordinated with metal centers (ESI, Fig. S5a†). In the second type of binding, 5TIA is tetradented and only carboxylate groups of 5TIA are coordinated to the metal centers (ESI, Fig. S5b†). In the crystal structure the Ca–O bond distances range from 2.425(3) to 2.660(3) Å. The $Ca–O_{water}$ and $Ca–N_{triazole}$ bond distances are 2.428(3) and 2.544(3) Å, respectively. Eight coordination sites of Ca(II) ions are fulfilled by five 5TIA ligands and one water molecule (ESI, Fig. S5c†). Ca-5TIA-MOF contains 1D channels along the crystallographic *c* axis and the free triazole rings are facing towards the channel (ESI, Fig. S5e†). The solvent accessible void of Ca-5TIA-MOF was calculated using *PLATON*[25] and suggested a 21.1% void volume relative to the total crystal volume. However, this increased to 38.5% after removal of the electron densities of solvent molecules residing inside the pore. The pore diameter of the channel is 3.6 Å (this value is calculated by considering the van der Waals radii of the constituent atoms).

Thermal stability

We have prepared the Ca-5TIA-MOF at the gram scale to allow a detailed investigation of the aforementioned 3D structure and to examine the stability (chemical, thermal and mechanical), gas affinity and catalytic properties. Thermal gravimetric analysis (TGA) performed on the as-synthesized Ca-5TIA-MOF revealed that these compounds present high thermal stability (Fig. 4a). The TGA curve for Ca-5TIA-MOF showed a sharp weight-loss step of 15% (90–160 °C), corresponding to evaporation of water and organic molecules (DMF) absorbed on the surface and trapped inside the pores. This is followed by a weight-loss of 27% (330–400 °C) assigned to the collapse of the framework, which is also observed in the case of Ca-5TIA-xerogel (38% weight loss). Common weight-losses up to 800 °C are attributed to further decomposition of the organic ligand in both systems. As for other Ca-MOFs, the final residual is attributed to calcium oxide. From the TGA traces it has been observed that solvent removal at Ca-5TIA-Gel happens over a broader temperature range (gradual weight-loss of 15% between 30 and 160 °C) because solvent molecules are loosely bound in the gel state, whereas in the crystalline Ca-5TIA-MOF, the solvent entrapped inside the pores leaves the framework over a much narrow temperature range.

Powder X-ray diffraction

In order to confirm the phase purity of the bulk materials, powder X-ray diffraction (PXRD) experiments were carried out

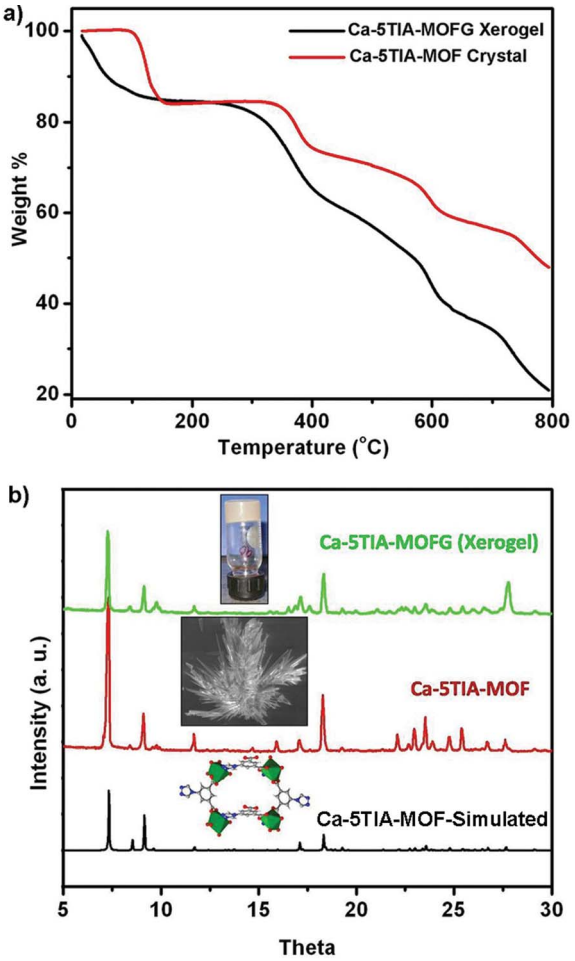

Fig. 4 (a) TGA traces of Ca-5TIA-xerogel (black) and Ca-5TIA-MOF (red). (b) Comparison of PXRD patterns of the Ca-5TIA-xerogel (green) and Ca-5TIA-MOF (red) with the simulated pattern from the single-crystal structure (black).

on Ca-5TIA-MOF as well as Ca-5TIA-xerogel (Fig. 4b). All major peaks of experimental PXRD of Ca-5TIA-xerogel and Ca-5TIA-MOF are well matched with simulated PXRD of Ca-5TIA-MOF, indicating reasonably crystalline phase purity.[36] There are some extra low intensity peaks that have been observed in Ca-5TIA-xerogel which may be due to the unreacted starting materials trapped inside the gel network. Despite these similarities, it seems unlikely that the MOF structure is fully retained in the gel materials. In fact, the absence of additional water during gelation as well as the influence of the counteranion in the stabilization of the gel materials point out a gelation mechanism in which the gelator agent is not the intact self-assembled 3D porous MOF. In this sense, no gels could be formed upon sonication of the MOF material in DMF, whereas the *in situ* coordination of the metal with the ligand and the solvation of the solvent molecules cannot be reproduced exactly from the xerogel (*i.e.* up to one week is necessary to obtain a partial gel from the corresponding xerogel material) either because of some structural change (not observable by PXRD) that occurs during the evaporation of the solvent or because of the insoluble nature of the metal-complex system, which prevents the right

accommodation of the solvent molecules that is necessary for the gelation phenomena. Moreover, we performed *in situ* variable temperature PXRD (VT-PXRD) of Ca-5TIA-Gel in order to understand the phase changes that might take place with increasing temperature (see Fig. S16†). *In situ* VT-PXRD patterns of Ca-5TIA-Gel collected at different temperatures (25 °C to 200 °C with a periodic interval of 25 °C) showed that the amorphous gel phase starts converting to a crystalline xerogel phase at around 100 °C. This suggests that the Ca-acetate-5TIA based gel (amorphous phase) can be irreversibly converted, upon removal of solvent, into a crystalline xerogel phase. Small differences in the intensities of the reflections are observed at higher temperatures because of the removal of residual solvent molecules. These results also support the premise that both the Ca-5TIA 3D MOF and the xerogel systems possess, at least, some common structural elements.

Morphological characterization

Scanning electron microscope (SEM) and transmission electron microscope (TEM) images of Ca-5TIA-MOF and Ca-5TIA-Gel were recorded in order to gain insights about the microstructure of the materials. Gel formation usually comprises the formation of 1D aggregates, which further undergo entanglement to form the 3D-network.[9] In the case of Ca-5TIA-Gels, the experimental protocol used to prepare the organogels showed a remarkable influence on the morphology of the 3D microfiber like-networks. For example, the use of sonication in order to disperse the gelator system seems to promote the formation of fibrillar networks of much higher homogeneity and high aspect ratio regardless of the processing temperature (Fig. 5a–d *vs.* e–i). Interestingly, the use of 25% less ligand with respect to $Ca(OAc)_2$ induced the formation of much denser and highly entangled rope-like structures, especially at high processing temperatures, with fiber diameters ranging between 0.5 and 10 μm (Fig. 5j–l). On the other hand, extended periods of heating also caused the evolution of well-defined fibrillar clusters towards a more compact material without visible bundles (Fig. 5f and g *vs.* h). The fibrillar evolution of the gel microstructure with increasing temperature was also confirmed when the samples were allowed to stand at 4 °C upon initial sonication, leading to a cobbled paving rather than a developed fibrillar surface (Fig. 5i).

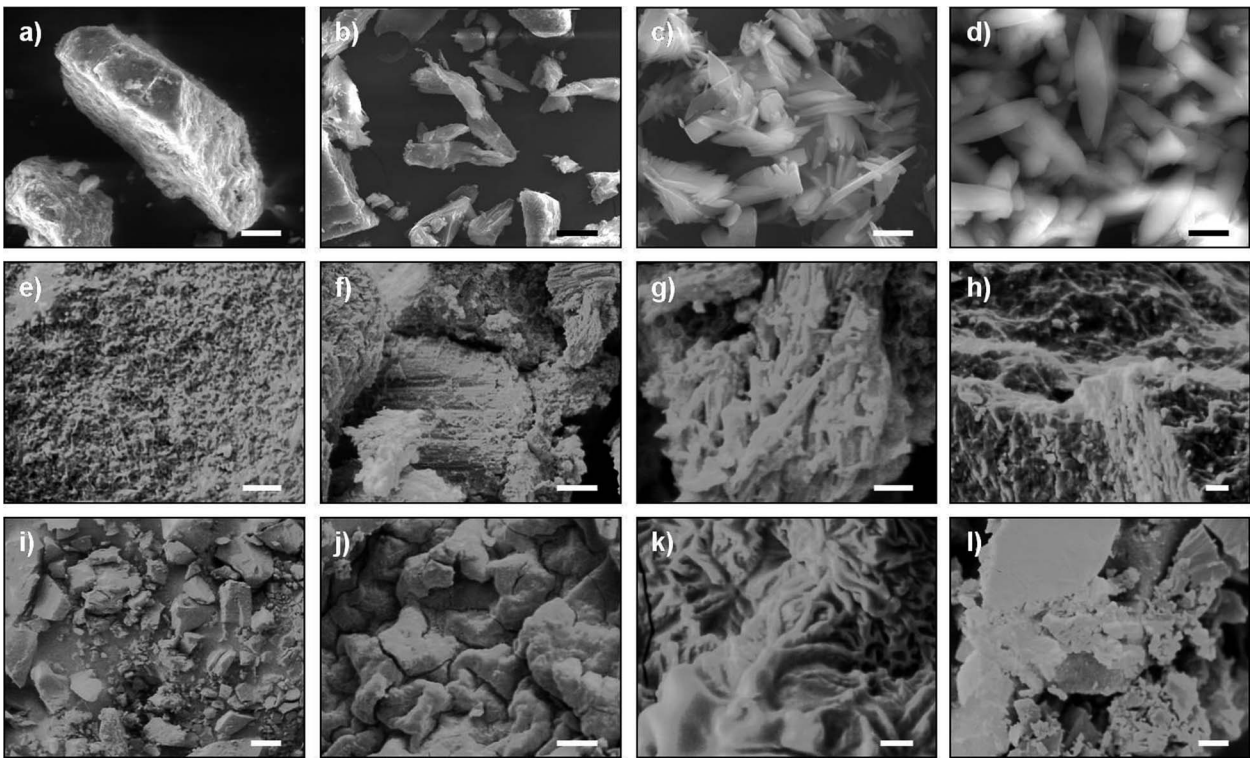

Fig. 5 SEM images of Ca-5TIA-Gels prepared in 1 mL DMF under different conditions: (a) 0.2 mmol $Ca(OAc)_2$ + 0.2 mmol 5TIA sonication at RT for 15 min, then standing at 30 °C → peach coloured gel (scale bar = 50 μm); (b) 0.2 mmol $Ca(OAc)_2$ + 0.2 mmol 5TIA sonication at RT for 15 min, then standing at 60 °C inside the oven → peach coloured gel (scale bar = 30 μm); (c) 0.2 mmol $Ca(OAc)_2$ + 0.2 mmol 5TIA sonication at RT for 15 min, then standing at 90 °C inside the oven → peach coloured gel (scale bar = 5 μm); (d) 0.2 mmol $Ca(OAc)_2$ + 0.2 mmol 5TIA sonication at RT for 15 min, then standing at 120 °C inside the oven → bright yellow coloured gel (scale bar = 10 μm); (e) 0.1 mmol $Ca(OAc)_2$ + 0.1 mmol 5TIA, sonication at RT for 15 min, then standing at RT → peach coloured gel (scale bar = 2 μm); (f and g) 0.1 mmol $Ca(OAc)_2$ + 0.1 mmol 5TIA, sonication at RT for 15 min, then heating at 120 °C in an oil bath for 2 h (scale bars = 5 and 2 μm, respectively); (h) 0.1 mmol $Ca(OAc)_2$ + 0.1 mmol 5TIA, sonication at RT for 15 min, then heating at 120 °C in an oil bath for 20 h → yellow coloured gel (scale bar = 2 μm); (i) 0.1 mmol $Ca(OAc)_2$ + 0.1 mmol 5TIA, sonication at RT for 15 min, then standing at 4 °C (scale bar = 100 μm); (j and k) 0.1 mmol $Ca(OAc)_2$ + 0.075 mmol 5TIA, sonication at RT for 15 min, then heating at 120 °C in an oil bath for 3 h → bright yellow coloured gel (scale bars = 20 and 1 μm, respectively); (l) 0.1 mmol $Ca(OAc)_2$ + 0.075 mmol 5TIA, sonication at RT for 15 min, then heating at 60 °C in an oil bath for 2.5 h → bright peach coloured gel (scale bar = 5 μm).

Infrared studies

Fourier transform infrared (FT-IR) spectra of the Ca-5TIA-Gel, Ca-5TIA-xerogel and Ca-5TIA-MOF appear to be virtually identical (Fig. 6a). This suggests that the internal structure of the Ca-5TIA-Gel was preserved during the preparation of its Ca-5TIA-xerogel, and has some resemblance to the crystalline Ca-5TIA-MOF. FT-IR spectra confirmed the presence of carboxylate groups in the coordination sphere of the metal and suggest that at least >95% of the carboxylic groups of 5TIA are deprotonated in the MOF materials. In this regard, the 5TIA ligand shows the C=O stretching frequency of free aromatic carboxylic acid at *ca.* 1699 cm^{-1}. When the carboxylic acid coordinates to the metal atoms, the C=O stretching frequency shifted to lower frequencies (*ca.* 1550 cm^{-1}), which is clearly observed in Ca-5TIA-Gel, Ca-5TIA-xerogel and Ca-5TIA-MOF. It is also expected that the C=O stretching frequency and the coordinated triazole stretching frequency are overlapped in the range of 1540–1550 cm^{-1}.

Gas adsorption

Ca-5TIA-MOF did not show nitrogen (N_2) uptake because the aperture size (3.6 Å) of the micropores is almost equivalent to the kinetic diameter of N_2 (3.6 Å). The kinetic diameter of N_2 (3.65 Å) is larger than the pore size of Ca-5TIA-MOF (3.6 Å) and N_2 molecules have, in addition, low kinetic energy at 77 K. As a result, N_2 molecules are unable to enter through the small pores of Ca-5TIA-MOF. However, it is able to take up carbon dioxide (CO_2). Unlike the transition metal based (*i.e.* Zn, Cu, Co and Ni) MOFs, CO_2 adsorption properties of Ca-MOFs have seldom been reported[18n,m] However, Ca-5TIA-MOF is able to take up CO_2 (3.4 Å) as it has a smaller kinetic diameter than the MOF pore aperture size. The CO_2 adsorption properties of Ca-5TIA-MOF and Ca-5TIA-xerogel are shown in Fig. 6b. Ca-5TIA-MOF and Ca-5TIA-xerogel show reversible type-I CO_2 adsorption isotherms at 298 K. Ca-5TIA-MOF and Ca-5TIA-xerogel adsorb 1.12 and 1.45 mmol g^{-1} of CO_2 at 298 K and 1 atm pressure. It is noteworthy that Ca-5TIA-xerogel shows 20% increase in CO_2 adsorption compared to the crystalline Ca-5TIA-MOF. This result remained consistent after repeated experiments. At this moment, we do not have a clear explanation for this anomalous behaviour, and we are carrying out detailed investigations along this line. It is noteworthy that despite several reports on Ca based MOFs in the literature, there exist only two Ca-based MOFs [$Ca(ptaH)(H_2O)]\cdot 6H_2O$:[18n] 0.8 mmol g^{-1} at 293 K, CYCU-1:[18m] 1.37 mmol g^{-1} at 298 K] that are able to take up CO_2. Our results indicate that the CO_2 uptake of Ca-5TIA-xerogel as well as Ca-5TIA-MOF is comparable to other reported Ca based MOFs.

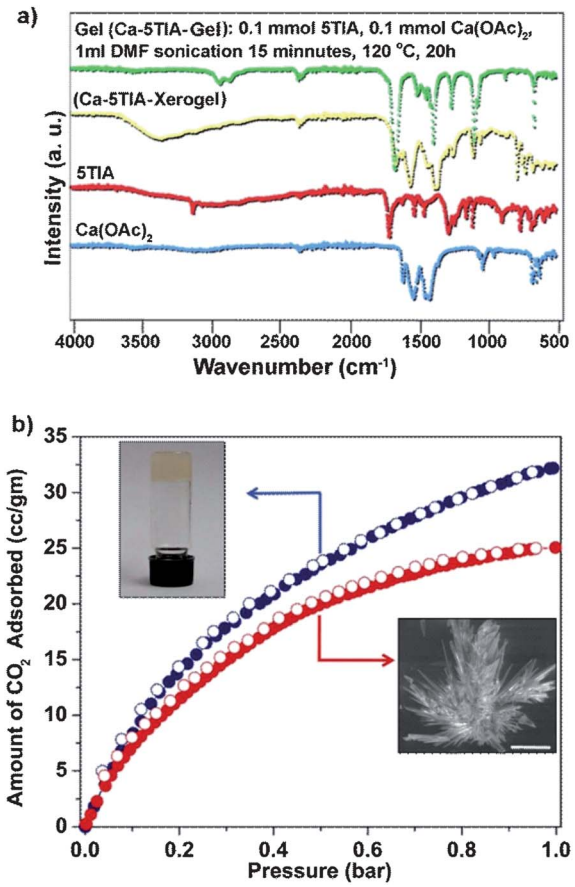

Fig. 6 (a) FTIR spectral patterns of $Ca(OAc)_2$ (blue), 5TIA ligand (red), Ca-5TIA-xerogel (yellow) and Ca-5TIA-Gel (green). (b) CO_2 adsorption isotherms below 1.0 bar for Ca-5TIA-xerogel (blue) and Ca-5TIA-MOF (red) at 298 K. Filled and open circles represent adsorption and desorption data, respectively.

Rheological measurements

We used rheology and small angle X-ray scattering to probe *in situ* both the nature and change in the gel structure during ageing. Rheological measurements were performed after intense pre-shearing to prepare a well-defined initial state for the sample. We observed that, even immediately after pre-shear (*viz.* at $t = 0$), the solid modulus, G', had a very weak frequency dependence (Fig. 7a). With ageing time, the solid modulus increased, but still maintained very weak frequency dependence ($G' \approx \omega^{0.045}$) over the entire 4-decades of frequency probed. The loss modulus (G'') was lower than the solid modulus, and had a minimum at high frequencies (ω between 10 and 100 rad s^{-1}, Fig. 7a). This indicates that the material has a network like structure, *viz.* it can be defined as a gel. However, the mechanical response was not dominated by the solid-like behaviour and there is significant dissipation (*viz.* G'' is not significantly lower than G', Fig. 7a and b). It is possible that the solid-like response is characteristic of the network structure formed by gelation of the particles of the Ca-5TIA, while the dissipation results from the associated solvent phase.[37] We can use the relation between the crosslink density and modulus for elastic networks, $G' = \rho\, k_B T$ (where ρ is the number density of network junctions, k_B is the Boltzmann constant and T is the temperature), to estimate the spacing between "network junctions" as *ca.* 2–3 nm.

Interestingly, we note that the solid modulus showed a slow, logarithmic thixotropic growth with ageing time, increasing about four-fold over 11 hours (Fig. 7a). This indicates the slow kinetics of the ageing process (Fig. 7a). At the end of the experiment, *viz.* after about 11 hours of ageing, the solid modulus of the gel was about 400 to 500 Pa. At the end of the ageing experiment, the gel was again subjected to intense steady shear at

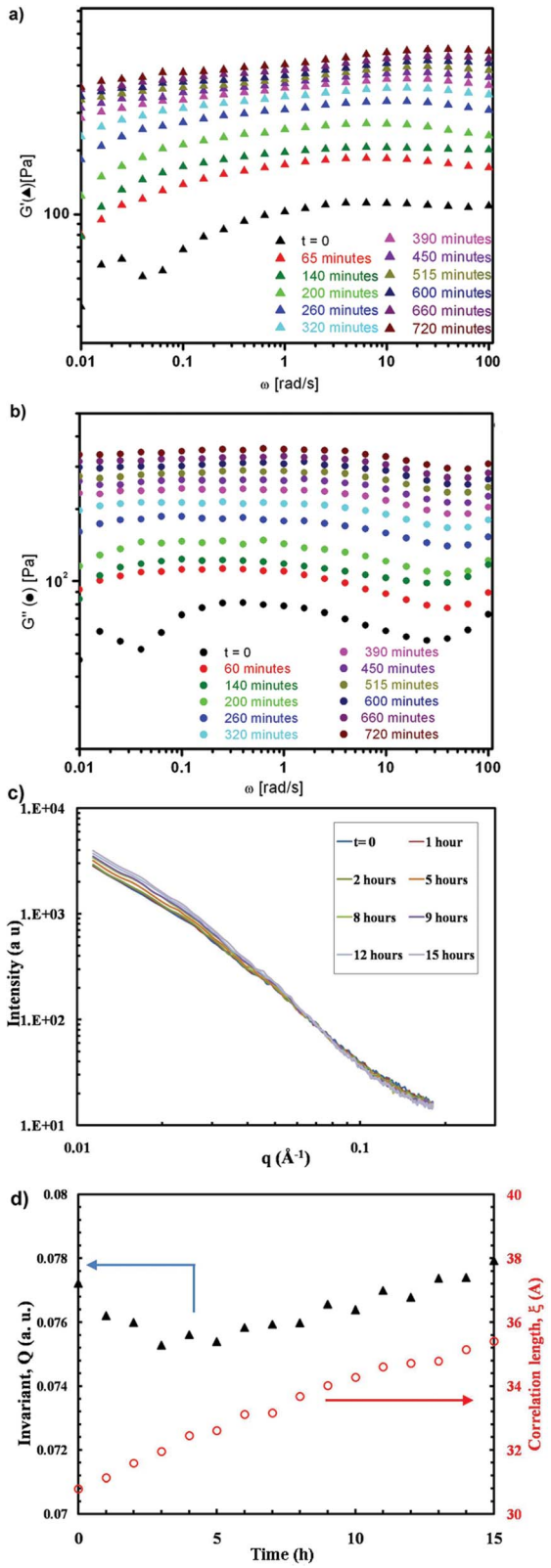

Fig. 7 Rheology and SAXS studies: (a) plot of the solid modulus (G') as a function of frequency (ω) with ageing time at RT using Couette geometry for Ca-5TIA-Gel. (b) Plot of the loss modulus (G'') as a function of frequency (ω) with ageing time at RT using Couette geometry for Ca-5TIA-Gel. (c) SAXS plot of q (Å^{-1}) as a function of scattering intensity (a.u.) with varying time. (d) SAXS plot of time (hours) as a function of correlation length (right-red) and invariant (left-black) plots for Ca-5TIA-Gel at 60 °C.

10 rad s^{-1}, and we observed a decrease in the gel modulus indicating a break-down of the network structure. The material was observed to gel again on standing, suggesting that a weak attraction between the Ca-5TIA particles is responsible for the thixotropic behaviour observed. We observed that the thixotropic response of the Ca-5TIA-Gels is qualitatively independent of the processing temperature, which could make them attractive for potential biomedical applications.

In agreement with the gradual increase in the modulus, we observed that the gel microstructure, from small angle X-ray scattering, also evolves gradually with ageing time (Fig. 7c). We could use the scattering invariant to characterize a two-phase structure in a model-independent manner. As we did not have scattering data over the entire q range, we approximated the invariant Q as $\int q^2 I(q)\,dq$ from the experimental q_{min} to q_{max}. We observed that the scattering invariant did not show any significant systematic change with time (Fig. 7d). We can write the invariant, $Q = 2\pi^2 x(1 - x)\Delta\rho^2$, where x is the fraction of the Ca-TIA particle, $(1 - x)$ is the solvent fraction and $\Delta\rho$ is the difference in electron density between the Ca-5TIA and the solvent. Thus, our data indicate that there is no significant change with ageing time of $\Delta\rho$, *viz.* the particles do not appear to densify with ageing. Based on the structure observed from TEM (ESI, Fig. S7 and S8†),[34] we modelled the small angle X-ray scattering data as arising from a random two phase structure and fitted a Debye–Bueche model, as follows: $I = I_o/(1 + q^2\xi^2)^2 + I_B$, where ξ is a correlation length that characterizes the structure, and I_o and I_B are fitting constants where I_B represents a q-independent background. The fit to the data is reasonable, except at very low q and indicates that the correlation length, ξ, increases gradually from about 31 to 36 Å over an ageing time of 15 h (Fig. 7d). These values of ξ show reasonable correlation with the distance between network points estimated from the rheology data, and with the dimensions of the void space between the Ca-5TIA particles from TEM.

Catalytic performance

Finally, the performance of both Ca-5TIA-MOF and Ca-5TIA-Gel as heterogeneous catalysts was also tested for the atom-efficient hydrosilylation of benzaldehyde with diphenylsilane as Lewis-acid catalyzed model reaction [$PhCHO + Ph_2SiH_2 \rightarrow PhCH_2OSiHPh_2$]. The reactions were carried out in DMSO based on the above-mentioned stability of the Ca-5TIA-Gel. As has been described for other Ca-based MOFs,[18k,m] the key factors responsible for the catalytic conversion of small molecules are: (1) a low restriction in mass transport due to macroporosity of the catalyst, (2) the Lewis acid character of the calcium and (3) the presence of coordinated solvent molecules (*e.g.* DMF) in the structure of the catalyst, which offsets the acidity of the Ca(II) center and favours this way the exchange of coordinated water molecules by other hard bases like carbonyl oxygens. In agreement with recent observations albeit with somewhat lower efficiency,[18k,m] Ca-5TIA-MOF (10 mol%) catalyzed the hydrosilylation of benzaldehyde affording the expected silylated product up to 70% within 24 h (Fig. 8). Interestingly, in spite of

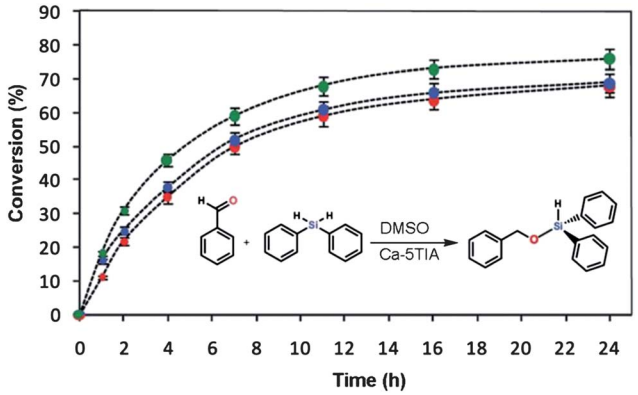

Fig. 8 Kinetic profile for the hydrosilylation of benzaldehyde catalyzed by Ca-5TIA-MOF (red), Ca-5TIA-xerogel (blue) and Ca-5TIA-Gel (green) (catalyst loading = 10 mol %).

the modest catalytic activity, the gel phase exhibited a modest higher activity in comparison to more rigid MOF and xerogel samples under comparable conditions ($TOFs_{1/2}$ (h^{-1}) = 1.09 (Ca-5TIA-Gel), 0.74 (Ca-5TIA-xerogel), 0.71 (MOF)). Such enhanced performance for the gel phase in comparison to the solid or crystalline phase has also been observed and discussed in other metallogels.[4g,9k] Nevertheless, considering the modest yields and differences observed between xerogel, gel and MOF materials, as well as the large size of the reactants in comparison to the pore size, the systems may likely operate as simple supported catalysts.

The absence of catalytic active species in solution, generated by potential leaching from the catalytic systems, was confirmed by a series of control experiments in which the reaction conditions (*i.e.* amount of catalyst, solvent, temperature and time) were simulated in the absence of reactants or in the presence of only one of the two reactants. After heating the padlocked catalyst in DMSO at 65 ± 5 °C for 1 h, the liquid phase was separated and used as a reaction medium for the hydrosilylation reaction of benzaldehyde with diphenylsilane under homogeneous conditions. No reaction was observed during the control experiments for both Ca-5TIA-MOF and Ca-5TIA-Gel, which ruled out leaching of active species, at least, above the minimum catalytic concentration. Moreover, no further conversion was observed when the catalysts were removed from the reactor after 1 h. Moreover, considering the estimated experimental error (*ca.* ±5%) only a minor detriment in the reaction conversion (Δ < 10%) was observed after the third run of the recycling experiments. The integrity of the catalysts was further confirmed by comparison of the PXRD patterns before and after the reaction.

Conclusion

In conclusion, we have demonstrated that 5TIA is a versatile ligand for the construction of new 3D Ca-based MOFs and stable metallogels. To the best of our knowledge this is the first report of Ca-based metallogels and 3D MOFs synthesized from the same organic and metal components. This is also the first porous Ca-based MOF that shows adsorption capacity for CO_2 at 1 atm pressure. Ca-5TIA-xerogel presents, on a molar basis, 20% higher CO_2 uptake than the crystalline Ca-5TIA-MOF. These materials are highly stable and retain crystallinity until 400 °C as confirmed by TGA. Ca-5TIA-Gel also showed an interesting thixotropic behaviour and it is characterized by a dynamic gel microstructure, which evolves with ageing time as demonstrated by rheological and X-ray scattering measurements. Experimental PXRD peaks of both Ca-5TIA-xerogel and Ca-5TIA-MOF matched reasonably well with simulated PXRD, suggesting the presence of, at least, some common structural elements in the 3D networks of both xerogel and crystalline phases, which was also supported by the similarities of the FT-IR spectra. However, the absence of extra water during gelation, the influence of the counteranion in the stabilization of the gels, and the failure to form the gel materials using the crystalline Ca-5TIA-MOF directly as a pure gelator agent point out a somewhat modified internal structure of the gels compared to the MOF materials. On the other hand, the synthesized materials also showed a modest catalytic activity towards the hydrosilylation of benzaldehyde with diphenylsilane, where slightly enhanced catalytic performance was found for the gel phase in comparison to the crystalline or xerogel materials. The ability of 5TIA to develop novel MOF and metallogel materials, including the corresponding MOF aerogels,[38] by coordination with other metal ions and counteranions or particles is currently under study in our laboratories and the results will be reported in due course.

Acknowledgements

A. M. and T. P. acknowledge CSIR for a Junior Research Fellowship. R. B. acknowledges NCL Director, for in-house project (MLP020626) and CSIR's XIth Five Year Plan Project (NWP0022-H) and Clean Coal Technology Project (NWP0021-A) for funding and Dr B. D. Kulkarni and Dr S. Sivaram for their encouragement. D. D. thanks Profs C. Cativiela and Marrero-Tellado for their support and technical assistance. R. B. thanks Dr Guruswamy Kumaraswamy for his assistance regarding the analysis of Rheology and SAXS data. Financial support from DST (SR/S1/IC-22/2009), UR (Anschubfinanzierung von Wissenschaftlichen Projekten-2011) and CSIC (PIE 200980I059) is also acknowledged.

References

1 (*a*) G. Férey, *Chem. Soc. Rev.*, 2008, **37**, 191; (*b*) A. U. Czaja, N. Trukhan and U. Müller, *Chem. Soc. Rev.*, 2009, **38**, 1284; (*c*) D. J. Tranchemontagne, J. L. Mendoza-Cortes, M. O'Keeffe and O. M. Yaghi, *Chem. Soc. Rev.*, 2009, **38**, 1257.

2 (*a*) H. L. Li, M. Eddaoudi, M. O'Keeffe and O. M. Yaghi, *Nature*, 1999, **402**, 276; (*b*) M. Eddaoudi, J. Kim, N. Rosi, D. Vodak, J. Wachter, M. O'Keeffe and O. M. Yaghi, *Science*, 2002, **295**, 469; (*c*) O. M. Yaghi, M. O'Keeffe, N. W. Ockwig, H. K. Chae, M. Eddaoudi and J. Kim, *Nature*, 2003, **423**, 705; (*d*) R. Matsuda, R. Kitaura, S. Kitagawa, Y. Kubota, R. V. Belosludov, T. C. Kobayashi, H. Sakamoto, T. Chiba, M. Takata, Y. Kawazoe and Y. Mita, *Nature*, 2005, **436**, 238; (*e*) J. L. C. Rowsell, E. C. Spencer, J. Eckert, J. A. K. Howard and O. M. Yaghi, *Science*, 2005, **309**, 1350; (*f*) D. Sun, S. Ma, Y. Ke, D. J. Collins and H.-C. Zhou, *J. Am. Chem. Soc.*, 2006, **128**, 3896; (*g*) J. L. C. Rowsell and O. M. Yaghi, *J. Am. Chem. Soc.*, 2006, **128**, 1304; (*h*) H. Noguchi, A. Kondo, Y. Hattori, H. Kajiro, H. Kanoh and K. Kaneko, *J. Phys. Chem. C*, 2007, **111**, 248; (*i*) R. E. Morris and P. S. Wheatley, *Angew. Chem., Int. Ed.*, 2008, **47**, 4966; (*j*) T. K. Trung, P. Trens, N. Tanchoux, S. Bourrelly, P. L. Llewellyn, S. Loera-Serna, C. Serre, T. Loiseau, F. Fajula and G. Férey, *J.*

Am. Chem. Soc., 2008, **130**, 16926; (*k*) H. Wang, J. Getzschmann, I. Senkovska and S. Kaskel, *Microporous Mesoporous Mater.*, 2008, **116**, 653; (*l*) D. Britt, D. Tranchemontagne and O. M. Yaghi, *Proc. Natl. Acad. Sci. U. S. A.*, 2008, **105**, 11623; (*m*) L. J. Murray, M. Dinca and J. R. Long, *Chem. Soc. Rev.*, 2009, **38**, 1294; (*n*) B. Chen, S. Xiang and G. Qian, *Acc. Chem. Res.*, 2010, **43**, 1115; (*o*) J. C. Tan, T. D. Bennett and A. K. Cheetham, *Proc. Natl. Acad. Sci. U. S. A.*, 2010, **107**, 9938; (*p*) J. C. Tan and A. K. Cheetham, *Chem. Soc. Rev.*, 2011, **40**, 1059.

3 (*a*) J. A. R. Navarro, E. Barea, J. M. Salas, N. Masciocchi, S. Galli, A. Sironi, C. O. Ania and J. B. Parra, *Inorg. Chem.*, 2006, **45**, 2397; (*b*) P. K. Thallapally, J. Tian, M. R. Kishan, C. A. Fernandez, S. J. Dalgarno, P. B. McGrail, J. E. Warren and J. L. Atwood, *J. Am. Chem. Soc.*, 2008, **130**, 16842; (*c*) L. Alaerts, M. Maes, L. Giebeler, P. A. Jacobs, J. A. Martens, J. F. M. Denayer, C. E. A. Kirschhock and D. E. De Vos, *J. Am. Chem. Soc.*, 2008, **130**, 14170; (*d*) Y. S. Bae, K. L. Mulfort, H. Frost, P. Ryan, S. Punnathanam, L. J. Broadbelt, J. T. Hupp and R. Q. Snurr, *Langmuir*, 2008, **24**, 8592; (*e*) M. Hartmann, S. Kunz, D. Himsl, O. Tangermann, S. Ernst and A. Wagener, *Langmuir*, 2008, **24**, 8634; (*f*) J.-P. Zhang and X.-M. Chen, *J. Am. Chem. Soc.*, 2008, **130**, 6010; (*g*) J.-R. Li, R. J. Kuppler and H.-C. Zhou, *Chem. Soc. Rev.*, 2009, **38**, 1477; (*h*) Y. S. Bae, O. K. Farha, J. T. Hupp and R. Q. Snurr, *J. Mater. Chem.*, 2009, **19**, 2131.

4 (*a*) K. Schlichte, T. Kratzke and S. Kaskel, *Microporous Mesoporous Mater.*, 2004, **73**, 81; (*b*) B. Gómez-Lor, E. Gutiérrez-Puebla, M. Iglesias, M. A. Monge, C. Ruiz-Valero and N. Snejko, *Chem. Mater.*, 2005, **17**, 2568; (*c*) A. Henschel, K. Gedrich, R. Kraehnert and S. Kaskel, *Chem. Commun.*, 2008, 4192; (*d*) F. Gándara, B. Gómez-Lor, E. Gutiérrez-Puebla, M. Iglesias, M. A. Monge, D. M. Proserpio and N. Snejko, *Chem. Mater.*, 2008, **20**, 72; (*e*) J. Y. Lee, O. K. Farha, J. Roberts, K. A. Scheidt, S. B. T. Nguyen and J. T. Hupp, *Chem. Soc. Rev.*, 2009, **38**, 1450; (*f*) L. Ma, C. Abney and W. Lin, *Chem. Soc. Rev.*, 2009, **38**, 1248; (*g*) J. Zhang, X. Wang, L. He, L. Chen, C. Y. Su and S. L. James, *New J. Chem.*, 2009, **33**, 1070.

5 (*a*) M. Vallet-Regí, F. Balas and D. Arcos, *Angew. Chem., Int. Ed.*, 2007, **46**, 7548; (*b*) A. Dupuis, N. Guo, Y. Gao, N. Godbout, S. Lacroix, C. Dubois and M. Skorobogatiy, *Opt. Lett.*, 2007, **32**, 109; (*c*) P. Horcajada, C. Serre, G. Maurin, N. A. Ramsahye, F. Balas, M. Vallet-Regí, M. Sebban, F. Taulelle and G. Férey, *J. Am. Chem. Soc.*, 2008, **130**, 6774; (*d*) W. Lin, W. Rieter and K. Taylor, *Angew. Chem., Int. Ed.*, 2009, **48**, 650; (*e*) O. Shekhah, H. Wang, M. Paradinas, C. Ocal, B. Schupbach, A. Terfort, D. Zacher, R. A. Fischer and C. Woll, *Nat. Mater.*, 2009, **8**, 481; (*f*) K. M. L. Taylor-Pashow, J. D. Rocca, Z. Xie, S. Tran and W. Lin, *J. Am. Chem. Soc.*, 2009, **131**, 14261; (*g*) N. J. Hinks, A. C. McKinlay, B. Xiao, P. S. Wheatley and R. E. Morris, *Microporous Mesoporous Mater.*, 2010, **129**, 330.

6 (*a*) B. L. Chen, L. B. Wang, F. Zapata, G. D. Qian and E. B. Lobkovsky, *J. Am. Chem. Soc.*, 2008, **130**, 6718; (*b*) B. L. Chen, L. B. Wang, Y. Q. Xiao, F. R. Fronczek, M. Xue, Y. J. Cui and G. D. Qian, *Angew. Chem., Int. Ed.*, 2009, **48**, 500; (*c*) J. R. Long and O. M. Yaghi, *Chem. Soc. Rev.*, 2009, **38**, 1213; (*d*) Z. Xie, L. Ma, K. E. deKrafft, A. Jin and W. Lin, *J. Am. Chem. Soc.*, 2010, **132**, 922.

7 K. S. Park, Z. Ni, A. P. Côté, J. Y. Choi, R. D. Huang, F. J. Uribe-Romo, H. K. Chae, M. O'Keeffe and O. M. Yaghi, *Proc. Natl. Acad. Sci. U. S. A.*, 2006, **103**, 10186.

8 S. Han, Y. Wei, C. Valente, R. S. Forgan, J. J. Gassensmith, R. A. Smaldone, H. Nakanishi, A. Coskun, J. F. Stoddart and B. A. Grzybowski, *Angew. Chem., Int. Ed.*, 2011, **50**, 276.

9 (*a*) D. J. Abdallah and R. G. Weiss, *Adv. Mater.*, 2000, **12**, 1237; (*b*) L. A. Estroff and A. D. Hamilton, *Chem. Rev.*, 2004, **104**, 1201; (*c*) N. M. Sangeetha and U. Maitra, *Chem. Soc. Rev.*, 2005, **34**, 821; (*d*) M. George and R. G. Weiss, *Acc. Chem. Res.*, 2006, **39**, 489; (*e*) S. Ray, A. K. Das and A. Banerjee, *Chem. Mater.*, 2007, **19**, 1633; (*f*) P. Dastidar, *Chem. Soc. Rev.*, 2008, **37**, 2699; (*g*) A. Ajayaghosh, V. K. Praveen and C. Vijayakumar, *Chem. Soc. Rev.*, 2008, **37**, 109; (*h*) A. R. Hirst, B. Escuder, J. F. Miravet and D. K. Smith, *Angew. Chem., Int. Ed.*, 2008, **47**, 8002; (*i*) A. Pal, H. Basit, S. Sen, V. K. Aswal and S. Bhattacharya, *J. Mater. Chem.*, 2009, **19**, 4325; (*j*) S. Samai, J. Dey and K. Biradha, *Soft Matter*, 2011, **7**, 2121; (*k*) D. D. Díaz, D. Kühbeck and R. J. Koopmans, *Chem. Soc. Rev.*, 2011, **40**, 427; (*l*) C. D. Jones, J. C. Tanb and G. O. Lloyd, *Chem. Commun.*, 2012, **48**, 2110.

10 B. Xing, M.-F. Choi and B. Xu, *Chem. Commun.*, 2002, 362.

11 (*a*) S. J. Novick and J. S. Dordick, *Chem. Mater.*, 1998, **10**, 955; (*b*) B. G. Xing, M. F. Choi and B. Xu, *Chem.–Eur. J.*, 2002, **8**, 5028; (*c*) J. F. Miravet and B. Escuder, *Chem. Commun.*, 2005, 5796; (*d*) Q. G. Wang, Z. M. Yang, X. Q. Zhang, X. D. Xiao, C. K. Chang and B. Xu, *Angew. Chem., Int. Ed.*, 2007, **46**, 4285; (*e*) T. Tu, W. Assenmacher, H. Peterlik, R. Weisbarth, M. Nieger and K. H. Dötz, *Angew. Chem., Int. Ed.*, 2007, **46**, 6368; (*f*) Q. G. Wang, Z. M. Yang, Y. Gao, W. W. Ge, L. Wang and B. Xu, *Soft Matter*, 2008, **4**, 550; (*g*) J. Zhang, X. Wang, L. He, L. Chen, C. Y. Su and S. L. James, *New J. Chem.*, 2009, **33**, 1070.

12 (*a*) M. Shirakawa, N. Fujita, T. Tani, K. Kanekob and S. Shinkai, *Chem. Commun.*, 2005, 4149; (*b*) S. Kume, K. Kuroiwa and N. Kimizuka, *Chem. Commun.*, 2006, 2442; (*c*) W. L. Leong, S. K. Batabyal, S. Kasapis and J. J. Vittal, *Chem.–Eur. J.*, 2008, **14**, 8822; (*d*) A. Saha, S. Manna and A. K. Nandi, *Chem. Commun.*, 2008, 3732; (*e*) S. K. Batabyal, W. L. Leong and J. J. Vittal, *Langmuir*, 2010, **26**, 7464.

13 (*a*) H. Z. Bu, A. M. English and S. R. Mikkelsen, *Anal. Chem.*, 1996, **68**, 3951; (*b*) L. Yang, S. S. Saavedra and N. R. Armstrong, *Anal. Chem.*, 1996, **68**, 1834; (*c*) H. Suzuki and A. Kumagai, *Biomacromolecules*, 2004, **5**, 486; (*d*) C. D. Geary, I. Zudans, A. V. Goponenko, S. A. Asher and S. G. Weber, *Anal. Chem.*, 2005, **77**, 185; (*e*) M. Honda, K. Kataoka, T. Seki and Y. Takeoka, *Langmuir*, 2009, **25**, 8349.

14 (*a*) O. Roubeau, A. Colin, V. Schmitt and R. Clérac, *Angew. Chem., Int. Ed.*, 2004, **43**, 3283; (*b*) M. R. Lohe, M. Rose and S. Kaskel, *Chem. Commun.*, 2009, 6056; (*c*) P. J. Bracher, M. Gupta, E. T. Mack and G. M. Whitesides, *ACS Appl. Mater. Interfaces*, 2009, **1**, 1807; (*d*) Y. Liao, L. He, J. Huang, J. Zhang, L. Zhuang, H. Shen and C. Y. Su, *ACS Appl. Mater. Interfaces*, 2010, **2**, 2333.

15 (*a*) K. Tsuchiya, Y. Orihara, Y. Kondo, N. Yoshino, T. Ohkubo, H. Sakai and M. Abe, *J. Am. Chem. Soc.*, 2004, **126**, 12282; (*b*) S. Kawano, N. Fujita and S. Shinkai, *J. Am. Chem. Soc.*, 2004, **126**, 8592.

16 (*a*) M. Shirakawa, N. Fujita, T. Tani, K. Kaneko, M. Ojima, A. Fujii, M. Ozaki and S. Shinkai, *Chem.–Eur. J.*, 2007, **13**, 4155; (*b*) S. K. Batabyal, A. M. P. Peedikakkal, S. Ramakrishna, C. H. Sow and J. J. Vittal, *Macromol. Rapid Commun.*, 2009, **15**, 1356.

17 D. S. Tsekova and V. B. Stoyanova, *Bulg. Chem. Commun.*, 2009, **41**, 149.

18 (*a*) M. J. Platers, R. A. Howie and A. Roberts, *Chem. Commun.*, 1997, 893; (*b*) Z. Fei, T. J. Geldbach, R. Scopelliti and P. J. Dyson, *Inorg. Chem.*, 2006, **45**, 6331; (*c*) C. Volkringer, T. Loiseau, G. Férey, J. E. Warren, D. S. Wragg and R. E. Morris, *Solid State Sci.*, 2007, **9**, 455; (*d*) Q. Shuai, S. Chen and S. Gao, *Inorg. Chim. Acta*, 2007, **360**, 1381; (*e*) K. Aliouane, N. Rahahlia, A. Guehria-Laidoudi, S. Dahaoui and C. Lecomte, *Acta Crystallogr., Sect. E: Struct. Rep. Online*, 2007, **63**, m1834; (*f*) C. Volkringer, J. Marrot, G. Férey and T. Loiseau, *Cryst. Growth Des.*, 2008, **8**, 685; (*g*) C. A. Williams, A. J. Blake, C. Wilson, P. Hubberstey and M. Schröder, *Cryst. Growth Des.*, 2008, **8**, 911; (*h*) P. D. C. Dietzel, R. Blom and H. Z. Fjellvag, *Z. Anorg. Allg. Chem.*, 2009, **635**, 1953; (*i*) A. E. Platero-Prats, V. A. de la Peña-O'Shea, M. Iglesias, N. Snejko, A. Monge and E. Gutiérrez-Puebla, *ChemCatChem*, 2010, **2**, 147; (*j*) A. E. Platero-Prats, V. A. de la Peña-O'Shea, N. Snejko, A. Monge and E. Gutiérrez-Puebla, *Chem.–Eur. J.*, 2010, **16**, 11632; (*k*) A. E. Platero-Prats, M. Iglesias, N. Snejko, A. Monge and E. Gutiérrez-Puebla, *Cryst. Growth Des.*, 2011, **11**, 1750; (*l*) P.-C. Liang, H.-K. Liu, C.-T. Yeh, C.-H. Lin and V. Zima, *Cryst. Growth Des.*, 2011, **11**, 699; (*m*) C. T. Yeh, W. C. Lin, S. H. Lo, C. C. Kao, C. H. Lin and C. C. Yang, *CrystEngComm*, 2012, **14**, 1219; (*n*) S. Neogi, J. A. R. Navarro and P. K. Bharadwaj, *Cryst. Growth Des.*, 2008, **8**, 1554.

19 S. Harder, *Chem. Rev.*, 2010, **110**, 3853.

20 *SMART, Version 5.05*, Bruker AXS, Inc., Madison, Wisconsin, 1998.

21 *Bruker, SAINT-Plus (Version 7.03)*, Bruker AXS Inc., Madison, Wisconsin, USA, 2004.

22 G. M. Sheldrick, *SADABS (Version 2.03) and TWINABS (Version 1.02)*, University of Göttingen, Germany, 2002.

23 G. M. Sheldrick, *SHELXS 97*, University of Göttingen, Germany, 1997.

24 G. M. Sheldrick, *SHELXTL 97*. University of Göttingen, Germany, 1997.
25 A. L. Spek, *PLATON, A Multipurpose Crystallographic Tool*, Utrecht University, Utrecht, The Netherlands, 2005.
26 (*a*) F. Fages, *Angew. Chem., Int. Ed.*, 2006, **45**, 1680; (*b*) M. M. Pires and J. Chmielewski, *J. Am. Chem. Soc.*, 2009, **131**, 2706.
27 (*a*) D. Lässig, J. Lincke and H. Krautscheid, *Tetrahedron Lett.*, 2010, **51**, 653; (*b*) T. Panda, P. Pachfule and R. Banerjee, *Chem. Commun.*, 2011, **47**, 7674.
28 (*a*) E. Neofotistou, C. D. Malliakas and P. N. Trikalitis, *CrystEngComm*, 2010, **12**, 1034; (*b*) P. Thuéry and B. Masci, *CrystEngComm*, 2010, **12**, 2982; (*c*) Z. P. Deng, L. H. Huo, H. Y. Wang, S. Gao and H. Zhao, *CrystEngComm*, 2010, **12**, 1526.
29 (*a*) S. Kume, K. Kuroiwa and N. Kimizuka, *Chem. Commun.*, 2006, 2442; (*b*) M. Chen, S.-S. Chen, T.-A. Okamura, Z. Su, M.-S. Chen, Y. Zhao, W.-Y. Sun and N. Ueyama, *Cryst. Growth Des.*, 2011, **11**, 1901; (*c*) M. Chen, M.-S. Chen, T.-A. Okamura, M.-F. Lv, W.-Y. Sun and N. Ueyama, *CrystEngComm*, 2011, **13**, 3801; (*d*) J. F. Eubank, L. Wojtas, M. R. Hight, T. Bousquet, V. C. Kravtsov and M. Eddaoudi, *J. Am. Chem. Soc.*, 2011, **133**, 17532.
30 M. Takeuchi and S. Kageyama, *Colloid Polym. Sci.*, 2003, **281**, 1178.
31 D. J. Adams, K. Morris, L. Chen, L. C. Serpell, J. Bacsa and G. M. Day, *Soft Matter*, 2010, **6**, 4144.
32 (*a*) M. J. Kamlet, J. L. M. Abbout, M. H. Abraham and R. W. Taft, *J. Org. Chem.*, 1983, **48**, 2877; (*b*) R. M. C. Goncalves, A. M. N. Simoes, L. M. P. C. Albuquerque, M. Roses, C. Rafols and E. Bosch, *J. Chem. Res., Miniprint*, 1993, 1380; (*c*) M. El-Sayed, H. Müller, G. Rheinwald, H. Lang and S. Spange, *Monatsh. Chem.*, 2003, **134**, 361; (*d*) A. Natrajan and D. Wen, *Green Chem.*, 2011, **13**, 913.
33 W. Edwards, C. A. Lagadec and D. K. Smith, *Soft Matter*, 2011, **7**, 110.
34 See ESI† for details.
35 A. Y. Y. Tam, K. M. C. Wong and V. W. W. Yam, *Chem.–Eur. J.*, 2009, **15**, 4775.
36 (*a*) M. Ma, D. Zacher, X. Zhang, R. A. Fischer and N. M. Nolte, *Cryst. Growth Des.*, 2011, **11**, 185; (*b*) Q. Zhang, J. Zhang, Q. Y. Yu, M. Pan and C. Y. Su, *Cryst. Growth Des.*, 2010, **10**, 4076; (*c*) C. S. Carr and D. F. Shantz, *Chem. Mater.*, 2005, **17**, 6192.
37 V. Trappe and D. A. Weitz, *Phys. Rev. Lett.*, 2000, **85**, 449.
38 (*a*) M. R. Lohe, M. Rose and S. Kaskel, *Chem. Commun.*, 2009, 6056; (*b*) A. P. Nelson, O. K. Farha, K. L. Mulfort and J. T. Hupp, *J. Am. Chem. Soc.*, 2009, **131**, 458.